AD-A066 601 SYSTEMS SCIENCE AND SOFTWARE LA JOLLA CALIF F/G 17/6
A DYNAMIC MAGNETIC TECHNIQUE FOR SENSING BLOCK MOTION.(U)
APR 78 P COLEMAN DNA001-77-C-0297
UNCLASSIFIED SSS-R-78-3643 DNA-4599F NL

| OF |
AD
A066601

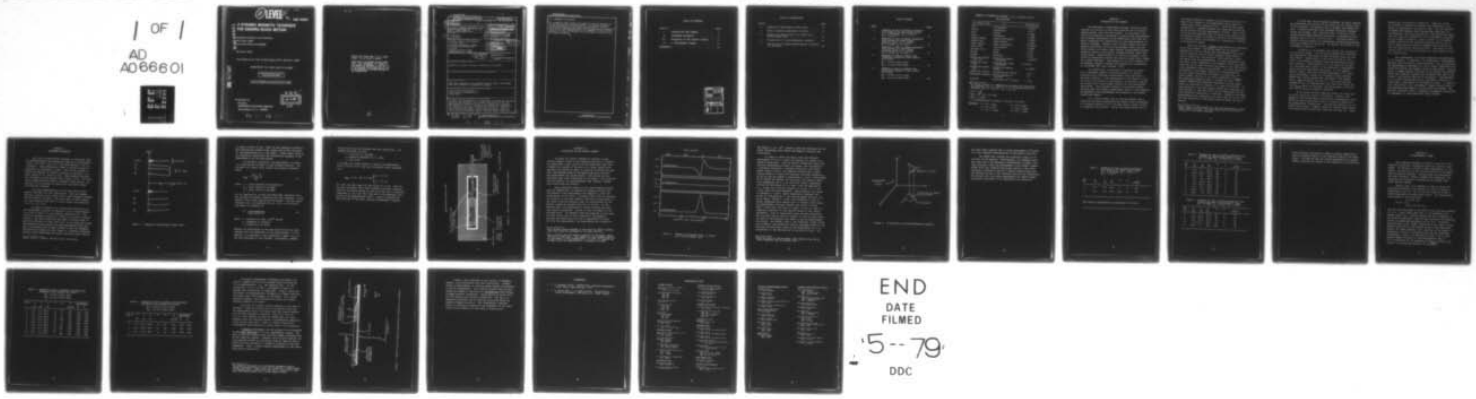

END
DATE
FILMED
5-79
DDC

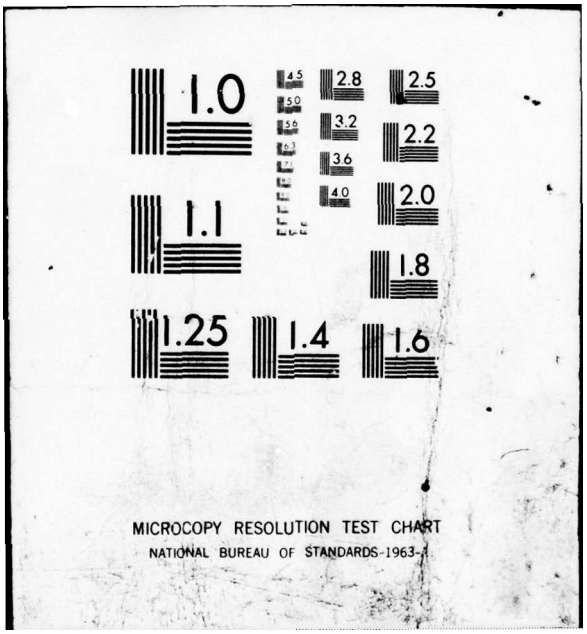
1.0
1.1
1.25
1.4
1.6
1.8
2.0
2.2
2.5
2.8
3.2
3.6
4.0
4.5
5.0
5.6
MICROCOPY RESOLUTION TEST CHART
NATIONAL BUREAU OF STANDARDS-1963-A

LEVEL II

DNA 4599F

A DYNAMIC MAGNETIC TECHNIQUE FOR SENSING BLOCK MOTION

Systems, Science and Software
P.O. Box 1620
La Jolla, California 92038

30 April 1978

Final Report for Period 22 August 1977—30 April 1978

CONTRACT No. DNA 001-77-C-0297

THIS WORK SPONSORED BY THE DEFENSE NUCLEAR AGENCY
UNDER RDT&E RMSS CODE B344077464 J34HAXSX31113 H2590D.

Prepared for
Director
DEFENSE NUCLEAR AGENCY
Washington, D. C. 20305

Destroy this report when it is no longer needed. Do not return to sender.

PLEASE NOTIFY THE DEFENSE NUCLEAR AGENCY, ATTN: TISI, WASHINGTON, D.C. 20305, IF YOUR ADDRESS IS INCORRECT, IF YOU WISH TO BE DELETED FROM THE DISTRIBUTION LIST, OR IF THE ADDRESSEE IS NO LONGER EMPLOYED BY YOUR ORGANIZATION.

627/14

UNCLASSIFIED

SECURITY CLASSIFICATION OF THIS PAGE (When Data Entered)

(19) REPORT DOCUMENTATION PAGE		READ INSTRUCTIONS BEFORE COMPLETING FORM
(18) 1. REPORT NUMBER: DNA 4599F	2. GOVT ACCESSION NO.	3. RECIPIENT'S CATALOG NUMBER
(6) 4. TITLE (and Subtitle): A DYNAMIC MAGNETIC TECHNIQUE FOR SENSING BLOCK MOTION.		(9) 5. TYPE OF REPORT & PERIOD COVERED: Final Report. 22 Aug 77—30 Apr 78,
		(14) 6. PERFORMING ORG. REPORT NUMBER: SSS-R-78-3643
(10) 7. AUTHOR(s): P. Coleman		(15) 8. CONTRACT OR GRANT NUMBER(s): DNA 001-77-C-0297
9. PERFORMING ORGANIZATION NAME AND ADDRESS: Systems, Science and Software, P.O. Box 1620, La Jolla, California 92038		(16) 10. PROGRAM ELEMENT, PROJECT, TASK AREA & WORK UNIT NUMBERS: NWET Subtask J34HAXSX311-13 (17) X311
(11) 11. CONTROLLING OFFICE NAME AND ADDRESS: Director, Defense Nuclear Agency, Washington, D.C. 20305		12. REPORT DATE: 30 April 1978
		13. NUMBER OF PAGES: 32
(12) 14. MONITORING AGENCY NAME & ADDRESS (if different from Controlling Office): 34p.		15. SECURITY CLASS (of this report): UNCLASSIFIED
		15a. DECLASSIFICATION/DOWNGRADING SCHEDULE

16. DISTRIBUTION STATEMENT (of this Report)

Approved for public release; distribution unlimited.

17. DISTRIBUTION STATEMENT (of the abstract entered in Block 20, if different from Report)

18. SUPPLEMENTARY NOTES

This work sponsored by the Defense Nuclear Agency under RDT&E RMSS Code B344077462 J34HAXSX31113 H2590D.

19. KEY WORDS (Continue on reverse side if necessary and identify by block number)

Block Motion Measurements
Ground Motion Instrumentation
Magnetometer

20. ABSTRACT (Continue on reverse side if necessary and identify by block number)

We report the development of a technique for dynamically sensing relative displacements; the intended application is for the measurement of block motion due to an underground explosion. The technique utilizes a permanent bar magnet and a magnetometer system located about a meter from the magnet. Relative motion between the magnet and magnetometer system leads to a time-varying magnetometer signal. The well-known properties → next page

DD FORM 1 JAN 73 1473 EDITION OF 1 NOV 65 IS OBSOLETE

388 507

UNCLASSIFIED

SECURITY CLASSIFICATION OF THIS PAGE (When Data Entered)

20. ABSTRACT (Continued)

of a magnetic dipole allows the magnet's relative position to be derived from the observed signals. We discuss hardening of the magnetometer to withstand ground "shock". We also show that the magnetometer system must measure both the magnetic field vector and (approximately) one component of the field's gradient in order to reliably infer the magnet's position from the observed signals.

TABLE OF CONTENTS

LIST OF ILLUSTRATIONS

LIST OF TABLES

SUMMARY OF CONVERSION FACTORS (U.S. to Metric Units) AND PREFIXES

To convert from	To	Multiply by
mils	millimeters	0.0254
inches	centimeters	2.54
feet	meters	0.3048
miles	kilometers	1.6093
square inches	square centimeters	6.4516
square feet	square meters	0.0929
cubic inches	cubic centimeters	16.38706
cubic feet	cubic meters	0.0283
gallons (U.S.)	liters	3.785
ounces	grams	28.349
pounds	kilograms	0.454
pounds per square inch, psi	newtons per square centimeter	0.6894757
pounds per cubic inch	kilograms per cubic centimeter	27,679.90
pounds per square foot	newtons per square meter	47.88026
inches per second	centimeters per second	2.54
Fahrenheit degrees	Celsius degrees or Kelvins[a]	5/9
kilotons	terajoules (10^{12} Joules)	4.183

[a] To obtain Celsius (C) temperature readings from Fahrenheit (F) readings, use $C = (5/9)(F - 32)$. To obtain Kelvin (K) readings, use $K = (5/9)(F - 32) + 273.15$.

$1\ Pa = 1\ \frac{N}{m^2}$

$1\ Bar = 10^5\ Pa = 14.5\ psi$

$1\ psi = 6.9\ KPa$

$1\ g$ = Acceleration of gravity = $32\ F/S^2 = 9.8\ m/s^2$

PREFIXES: $G = 10^9$ = giga $M = 10^6$ = mega

$K = 10^3$ = kilo $c = 10^{-2}$ = centi

$\mu = 10^{-6}$ = micro $n = 10^{-9}$ = nano

SECTION I
INTRODUCTION AND SUMMARY

The designers of deep-based strategic structures must consider the survival of both the structure and its access/communications links with the surface. In particular, the latter are especially vulnerable to large ground displacements. The interface experiments on the MIGHTY EPIC event were primarily concerned with observations of such displacements at a material boundary. However, even "uniform" media like tuff exhibit significant joints and slip-planes within the rock. Ground motion can induce large relative displacements between adjoining blocks of the medium, thereby breaking cables and access lines. Reported here is an effort to develop a technique for dynamically sensing the relative block motion caused by a nearby explosion. The approach is an active version of the passive, magnetic scheme, which worked very successfully on the MIGHTY EPIC test (Coleman, 1978).

For MIGHTY EPIC, the measuring technique utilized a set of permanent magnets installed pre-shot in vertical boreholes and a three-axis magnetometer used post-shot in adjacent boreholes. From observations of the magnetic field, $\vec{B}$, within a few meters of the magnets, the postshot location and orientation of each magnet relative to the magnetometer was derived. With accurate surveys of the preshot magnet positions and the postshot magnetometer holes, it was possible to determine total displacement and rotation in the volume around each magnet.

In an active system, one or more bar magnets and at least one tri-axial magnetometer per magnet would be emplaced in a preshot borehole, up to one meter apart, across a known or suspected slip surface. During the ground motion due to

the nearby explosion, changes in the relative position of a magnet with respect to its magnetometer would lead to a time-varying vector magnetic field. Given the well-known properties of a magnetic dipole, the time-varying position can be derived from the magnetometer signals. Such a technique has the advantages that it can be quite sensitive and the observed signal is directly related to the displacement of interest without the necessity of integrating a velocity or acceleration signal.

There are several a priori requirements for successful use of this scheme. The medium should be low magnetic permeability rock to ensure that the background due to the earth's magnetic field is quite uniform; large masses of iron or steel like rock bolts and rails must be at least ten meters from the magnetometer. At each measurement time, the three vector components of the magnetic field are determined and can be used to derive any three of the eight significant parameters defining the problem: the three Cartesian coordinates of the magnet relative to the magnetometer; the two angles describing the magnet's orientation, the dipole moment; and two of the three components of $\vec{B}_{EARTH}$.* The remaining parameters must be treated as known. For example, MIGHTY EPIC experience indicates that the dipole moment is unaffected by shocks of at least two kilobars. In some situations, one might safely assume that rotations are insignificant or that the motion is two dimensional and the third Cartesian coordinate is invariant. Currently available magnetometers have responses to at least 1000 Hz (3 db); thus the time resolution of the system would be about 350 microseconds.

*This allows for the possibility that the magnetometer itself might rotate; however, the total magnitude of the earth's background field stays constant.

As with most active measuring schemes, the major problems are protection and survival of the sensor and the signal cable. In this instance, the magnetometer is probably the weakest element. Previous experience with hardened electronic packages (Grine and Coleman, 1974) indicates that a void-free, fully potted system offers the best protection in acceleration environments up to 10^5 m/s^2 (10 kilo-"g's"). Contained within a stress isolating package, an acceleration hardened magnetometer would be suitable for field use. We discuss the details of the instrument in Section 2.

In Section 3, we consider the accuracy and reliability of the active scheme. For the passive MIGHTY EPIC technique, the magnetometer was placed at many different positions near each magnet. Observations of the vector $\vec{B}$ field at (typically) ten different locations then overdetermined the problem, allowing a least-squares fit to the data and allowing for inevitable small errors in the measured $\vec{B}$, magnetometer positioning and background variations. For the present dynamic scheme, each time resolved measurement of $\vec{B}$ (about every millisecond) allows us to determine three unknowns. MIGHTY EPIC results showed that rotations of the magnets were in <u>most</u> instances less than 5°. With the plausible assumption that the magnetometers also would not rotate and thus $\vec{B}_{EARTH}$ would be invariant, each measurement of $\vec{B}$ would allow us to derive the magnet's position.

As we tested the data reduction system, we found that the above ideas are correct in principle. However, the <u>errors</u> in the derived magnet position are unacceptabley large, given the known statistical errors in $\vec{B}$ and the magnet and the magnetometer orientations. Our detailed reduction of the MIGHTY EPIC results, recently completed, showed three magnets with statistically significant rotations of order 10°. These

magnets were in regions of large slip. Since our scheme is intended to monitor slip planes, our assumptions of no magnet or magnetometer rotations is weak. For the remaining 33 MIGHTY EPIC magnets, the rotations were less than ±5°. Unfortunately, even uncertainties of a few degrees are important when only one observation of $\vec{B}$ is available to uniquely derive a magnet's position. Small "errors" in the magnet's assumed orientation and strength allow the field to be fit with a magnet position which is mathematically correct but (for our application) physically wrong. The origin of this problem lies in the well-structured but quite symmetric form of a dipole field.

As a consequence, the active technique discussed above is not suitable. In Section 4, we investigate a "gradiometer" approach that would work in many instances. For this approach, two magnetometers separated by a ten to twenty centimeter distance would detect the magnetic field of each magnet. Mounted within a common package, rotations in the earth's field would affect both detectors equally and contribute much less to the errors in the derived position of the magnet. Unfortunately, all six field signals must be well recorded in order to reliably make a measurement of the magnet's motion. In spite of this complication, the "gradiometer" scheme could be used if time-resolved measurements of block motion are needed. The magnetic technique offers a completely independent alternative or complement to accelerometer/DX gauge systems.

SECTION II
INSTRUMENT HARDENING

For use in ground motion studies, an instrument must be hardened against the deleterious effects of high acceleration (~10^4 m/s^2, 1000 'g's') and high pressure (~10^8 Pa, 1 kilobar). High acceleration leads to relative motion of components and breakage of leads. This can be avoided by making the package as uniform in density as possible, i.e., there should be no internal voids. High pressure stresses the instrument's parts beyond their elastic limit. For electronic components and sensitive magnetic field sensors, the solution is to surround the gauge with a pressure vessel of sufficient strength.

Flux gate magnetometers are the best vector field sensors available for this application. They are compact, accurate, require little power, have a high frequency response and are readily available. The units that we used* contain all three sensing axes within a fully potted case measuring 3.2 x 3.5 x 12.1 cm.

In order to estimate the acceleration sensitivity of the magnetometer package, we mounted it and an accelerometer on a 0.64 cm thick, 12.2 cm diameter aluminum plate. The plate was dropped a distance of roughly 20 cm onto a concrete surface. The impact subjected the plate to maximum peak to peak accelerations of about 3x10^4 m/s^2 (3 kg) along the X axis. The resulting noise signals from the magnetometer were less than 8 milligauss peak to peak; Figure 1 gives two examples. The plate was wrapped with two layers of a magnetic shielding material which attenuated the earth's one half gauss field by

*Model 9200C-S, Develco, Mountain View, California.

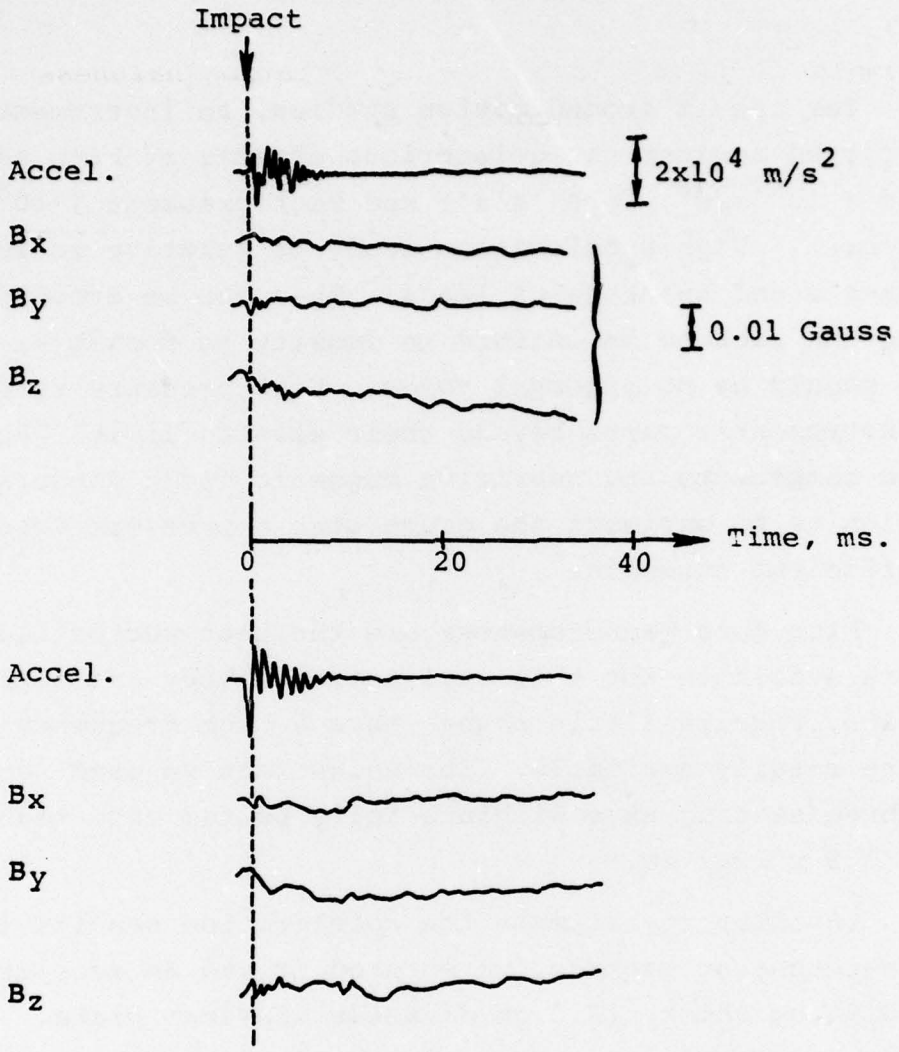

Figure 1. Examples of magnetometer shock tests.

at least a factor of ten. Thus, we were measuring primarily the acceleration induced noise rather than slight rotations of the magnetometer due to the impact. These simple tests do not completely demonstrate the acceleration hardness of the magnetometer, but are encouraging.

For pressure protection, the magnetometer is potted in a thick-walled cylinder of high strength material. The cylinder will remain fully elastic for external pressures below

$$P_{MAX} = \frac{Y(r_e^2 - r_i^2)}{2r_e^2} \qquad (1)$$

where Y = yield strength of the material,
r_e = outer radius of cylinder,
r_i = inner radius of cylinder.

For our application, we have the additional constraint that the cylinder not greatly attenuate the high frequency (~1 kHz) magnetic field which constitutes the signal. The skin depth (distance for an attenuation of 1/e, 0.37) of an infinite half-space of conductor is

$$d_s \sim \frac{c}{\sqrt{4\pi^2 \nu (9\times10^{17}/\rho)}} \qquad (2)$$

where c = velocity of light, 3×10^{10} cm/sec,
ν = frequency of interest,
ρ = resistivity in $\mu\Omega$-cm.

Because the wavelengths of the time varying $\vec{B}$ are so large compared with the dimensions of the gauge package (~10 cm), equation (2) represents a very conservative upper limit on the wall-thickness of the cylinder. Fortunately, INCONEL

alloys have both high strength and high resistivity. For INCONEL alloy 625, we find

$Y > 0.83$ GPa (8.3 kilobar),

μ = magnetic permeability = 1.0006,

$\rho = 129\ \mu\Omega$-cm.

A cylinder just large enough to contain the magnetometer with a 4.8 mm (3/16") wall will withstand static pressures up to

$$P_{MAX} = 0.14 \text{ GPa (1.4 kB)} \begin{cases} r_e = 2.7 \text{ cm} \\ r_i = 2.2 \text{ cm}. \end{cases}$$

At 1 kHz, the skin depth of this alloy is 1.8 cm. Thus the one half centimeter wall would attenuate the high frequency field of the moving magnet by much less than 23%, a magnitude comparable to the 3 db (29%) loss due to the bandwidth limitation of the magnetometer itself. Figure 2 sketches the main features of the shock resistant magnetometer package.

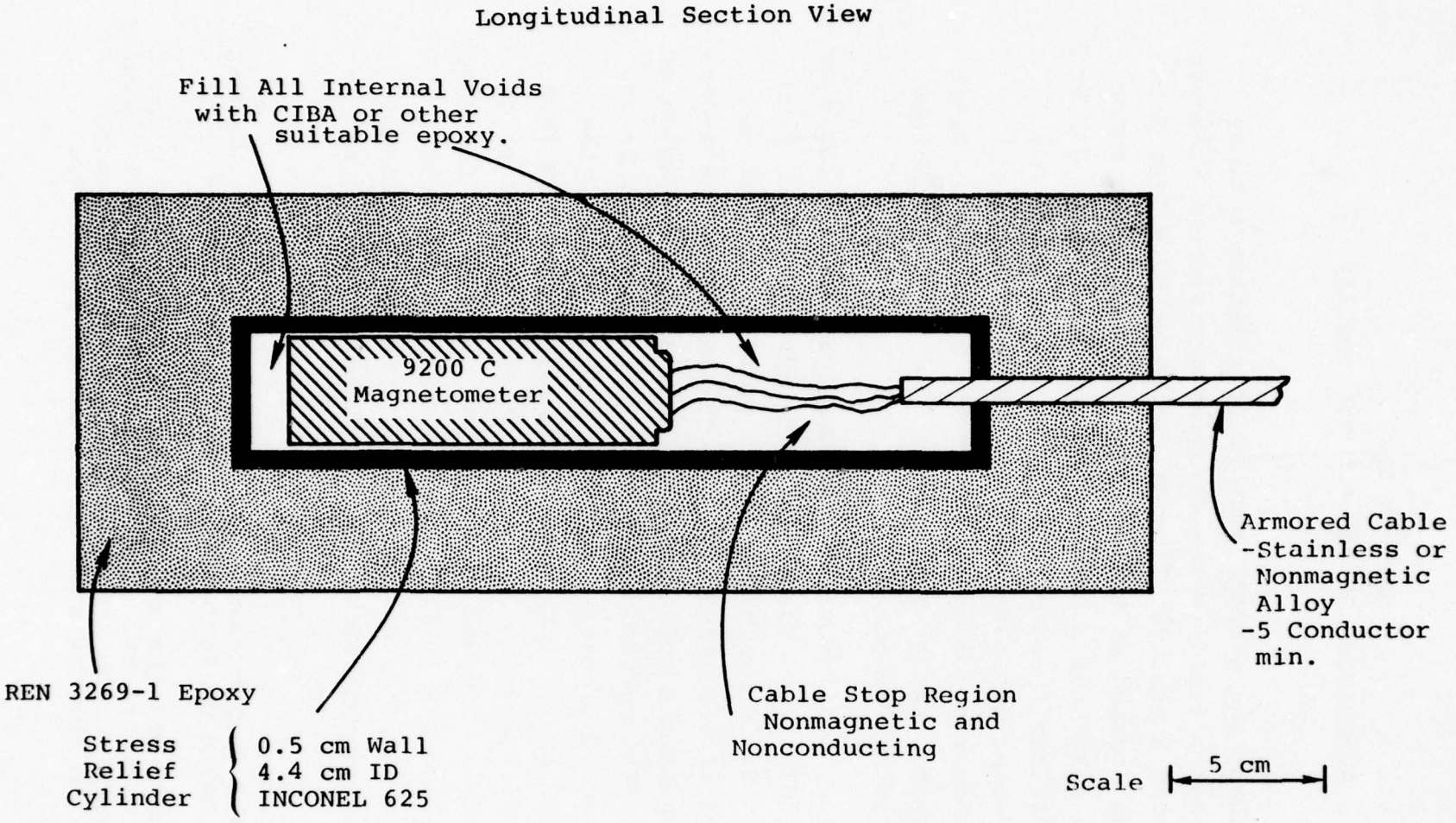

Figure 2. Shock resistant magnetometer canister.

SECTION III
EVALUATION OF THE DYNAMIC CONCEPT

To check the overall concept of relating a time-varying magnetic field to the changing position of a magnet, we constructed a test facility at the Green Farm Test Site. A magnet was located at the end of a 1 meter radius rotor and spun by a hydraulic motor at rates up to nearly 400 rpm; thus, the maximum speed of the magnet was about 40 m/s.* The magnetometer was placed nearby. This design has the advantage that three coordiantes of the magnet (two Cartesian and one angular) are simultaneously time varying, thereby fully exercising the concept.

With a modified version of our least-squares program used for MIGHTY EPIC, we derived the magnet's motion from the magnetic field measurements and compared it with the known motion of the rotor. To better than ±1/2%, we observed no variation in the peak magnetic field and no deviation of the rotor's derived position from its true position as the magnet's speed was changed from zero to 38 m/s. At the maximum rate, the magnetometer's signal risetime was less than seven milliseconds. Figure 3 gives an example of the recorded data.† The magnet's axis was parallel to the rotor; the spin vector was in the +Y direction; the magnet's strength was 52000 Gauss-cm^3 and it approached to within 48 cm of the magnetometer; the magnetometer was located in

---

*With several design changes in the rotor to reduce airdrag, this rate could be increased to at least 100 m/s.

†Rotor azimuth was the angular position of the magnet about the axis of the motor. Zero degrees is the closest approach of the magnet to the magnetometer. At 180°, the magnet was furthest from the magnetometer, a distance of 2.48m.

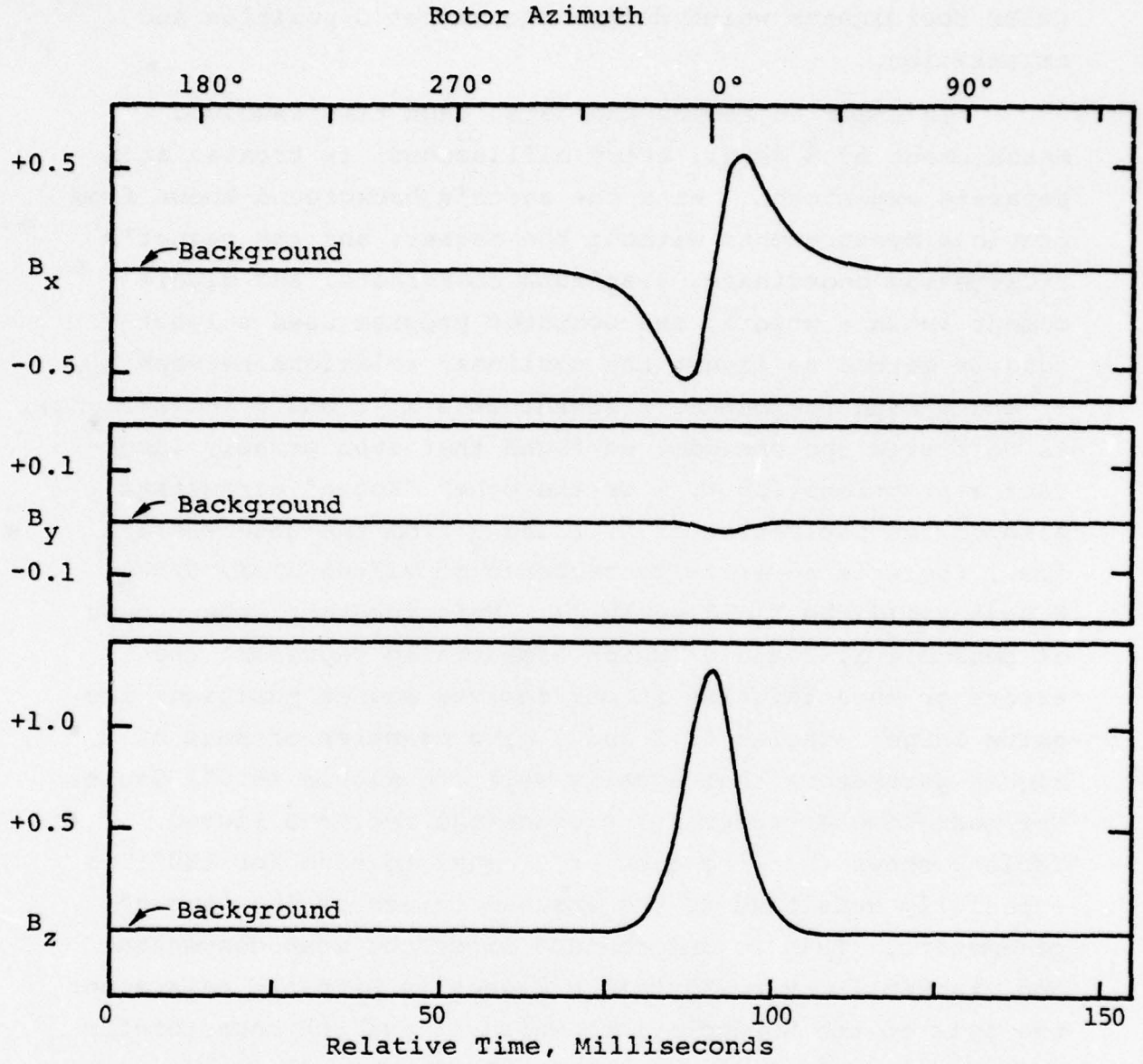

Figure 3. Example of observed field (in Gauss) for a moving magnet test.

the plane Y = +0.7 cm.[@] Figure 4 shows the Cartesian and angular coordinates which define the magnet's position and orientation.

In order to reduce the data, each time resolved measurement of $\vec{B}$ (e.g., every millisecond) is treated as a separate experiment. With the earth's background known from previous measurements without the magnet, and the magnet's Y Cartesian coordinate, ϕ azimuth coordinate, and dipole moment known a priori, the computer program used a least-squares method to invert the nonlinear relations between B_x, B_y and B_z and the magnet's coordinates X, Z and θ (colatitude). As we tested the program, we found that even grossly incorrect assumptions for Y, ϕ or the other "known" parameters allowed the derivation of X, Z and θ from the observed $\vec{B}$; i.e., there is an infinite sequence of values of X, Z and θ that yield the field measured. Unfortunately, the ranges of possible X, Z and θ (which essentially represent the errors or uncertainties in our derived magnet position) are quite large. Tables 1, 2 and 3 give examples of sets of magnet parameters that equally well (to within ±0.003 Gauss, the magnetometer accuracy) produce the vector $\vec{B}$ listed. Table 1 shows that the case of θ equal to zero (or 180°) is especially sensitive to the assumed values of the "known" parameters. This is unfortunate since the most convenient and practical way to install a magnet is with its axis along the axis of the borehole into which it and the magnetometer are placed. For Tables 2 and 3, the "observed" fields differ only slightly; the variations could be ascribed either to the accuracy and electronic noise of the magnetometer or to an uncertainty in the contribution of the earth's field. We

[@] With the rotor in the XZ plane, this explains why the B_y field component was not exactly zero.

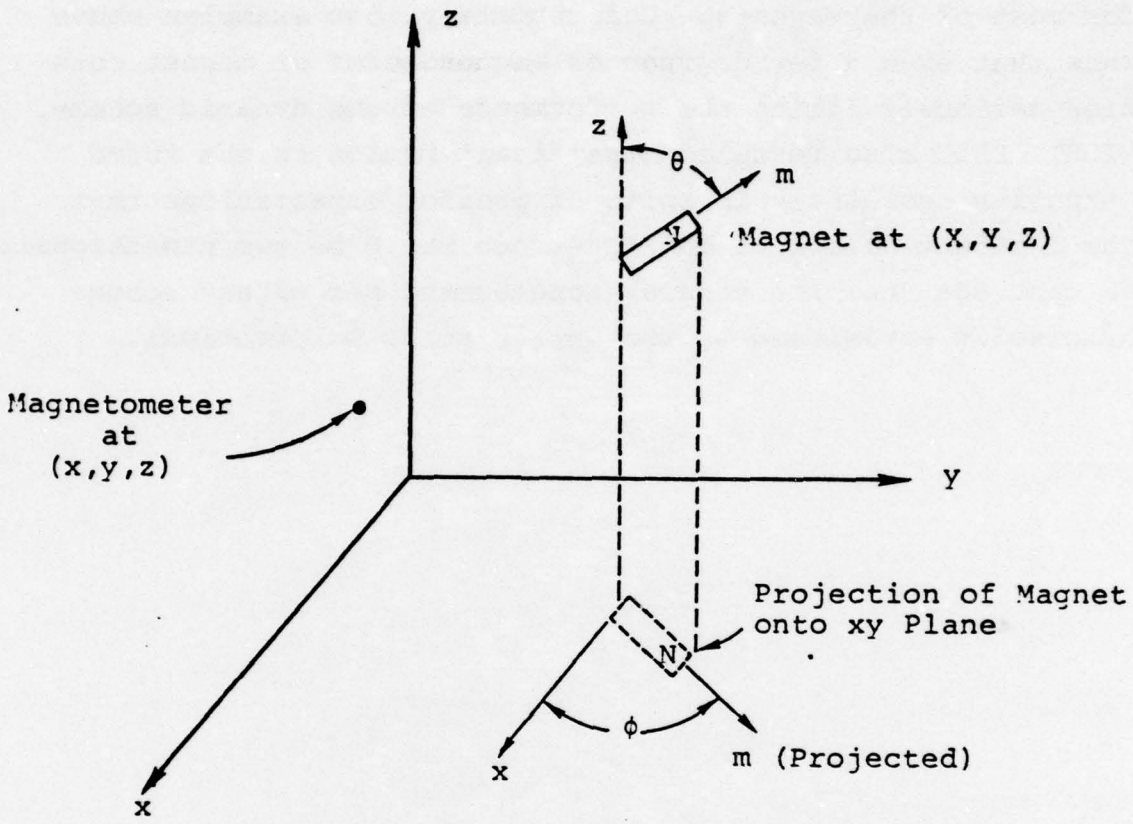

Figure 4. Illustration of three-dimensional geometry.

see from these examples that a single measurement of $\vec{B}$ leads to a very imprecise determination of the magnet's position.

Our MIGHTY EPIC results set rotational limits of ±5° for most of the magnets. Unfortunately, our examples above show that even a few degrees of magnetometer or magnet rotation seriously limits the performance of the dynamic scheme. MIGHTY EPIC also revealed significant motion in the third Cartesian coordinate in spite of preshot expectations that the dominant motion of the interface would be two dimensional. We conclude that the single magnetometer per magnet scheme originally envisioned is too imprecise to be practical.

Table 1. Examples of sets of magnet parameters that produce the same* vector field, B_x = 0.045 Gauss, B_y = 0.091 G, B_z = 1.155 G.

Set #	X cm	Y cm	Z cm	θ°	φ°	m kG-cm^3
1	1.0	2.0	50.0	0.	0.	50
2	9.5	2.0	48.2	32.0	0.	50

*To within an experimental uncertainty of ±0.003 G.

Table 2. Examples of sets of magnet parameters that produce the same vector magnetic field, B_x = -0.589G, B_y = 0.000G, B_z = 0.037G.

Set #	X cm	Y cm	Z cm	θ°	φ°	m kG-cm^3
1	1.0	0	50.0	90	0	50
2	-0.3	-14.1	48.0	88	-2	51
3	-0.3	14	48.0	88	2	51
4	1.6	0.0	50.3	91	0	51
5	0.7	23.8	42.6	91	2	49
6	0.6	-31.8	36.2	92	-2	50
7	-1.7	41.0	20.9	92	5	50
8	-22.6	3.0	45.8	43	5	50
9	16.4	3.0	47.2	121	-2	50

Table 3. Examples of sets of magnet parameters that produce the same vector magnetic field, B_x = -0.588G, B_y = 0.002G, B_z = 0.035G.

Set #	X cm	Y cm	Z cm	θ°	φ°	m kG-cm^3
1	1.0	2.2	50.0	90	0	50
2	-0.4	-13.1	47.8	88	-2	49
3	0.6	27.1	41.0	91	2	51
4	1.6	-17.3	46.4	92	-1	50
5	41.8	0	32.0	183	5	50

third Cartesian coordinate in spite of preshot expectations that the dominant motion of the interface would be two dimensional. We conclude that the single magnetometer per magnet scheme originally envisioned is too imprecise to be practical.

SECTION IV
A "GRADIOMETER" SCHEME

The problems discussed in Section 3 were due to the absence of sufficient information about the field of each magnet. By devoting a second triaxial magnetometer to each magnet, the precision of the derived position of the magnet would be greatly improved. We would have six measurements and eight unknowns. Based on MIGHTY EPIC experience, the constancy of the magnet's strength may be assumed; thus seven unknowns remain.

Tables 4 and 5 give examples of sets of magnet and background parameters that produce (to within an assumed magnetometer error of ±.003 G) the two values of $\vec{B}$ that a double magnetometer package would detect. The magnetometers were assumed to be at positions

$$(X,Y,Z) = \begin{cases} (0,0,0), \vec{B}_1 \\ (0,0,-20 \text{ cm}), \vec{B}_2 \end{cases}$$

and the total magnitude of the earth's field was held constant at 0.5 G. These tables show that if two parameters are assumed known (e.g., dipole strength and the X component of the earth's background), then the data determine the remaining magnet and background parameters fairly well. Plausible uncertainties in the "known" quantities do not lead to unreasonable variations in the derived values of the other parameters; for these examples, the Z position of the magnet is determined to within a centimeter and even the transverse coordinates, X and Y, are uncertain to only ±5 cm or less. Several degree rotations of the magnetometers lead to 0.01 G variations in the components of $\vec{B}_{EARTH}$ without great "errors" in the derived position of the magnet.

Table 4. Examples of sets of magnets and background parameters that produce the fields

$\vec{B}_1 = (0.131, 0.233, 1.418)$

$\vec{B}_2 = (0.118, 0.205, 0.898)$

Set #	X cm	Y cm	Z cm	θ°	φ°	m kG-cm^3	BACKGROUND X G	BACKGROUND Y G
1	0.7	2.1	69.6	-1	-19	161	.110	.190
2	4.3	2.2	69.3	10	3	161	.124	.190
3	0.4	4.8	69.3	-8	-78	161	.108	.200
4	1.5	-0.8	69.6	8	-80	161	.113	.180
5	-5.8	2.2	68.4	-19	0	158	.084	.190
6	0.8	2.6	68.2	-2	-80	152	.110	.192
7	7.4	-0.3	69.2	19	-20	165	.136	.180
8	-4.5	1.1	69.2	-16	11	161	.090	.185
9	1.1	1.6	68.7	1	-80	155	.110	.188

Table 5. Examples of sets of magnet and background parameters that produce the fields

$\vec{B}_1 = (0.293, -0.077, 1.252)$

$\vec{B}_2 = (0.179, +0.082, 0.846)$

Set #	X cm	Y cm	Z cm	θ°	φ°	m kG-cm^3	BACKGROUND X G	BACKGROUND Y G
1	7.6	-10.4	69.6	12	123	160	.102	.190
2	10.9	-10.2	69.5	10	80	160	.110	.190
3	6.7	-11.7	68.9	11	147	155	.100	.184

The double magnetometer technique also permits the use of a magnet with its axis aligned along the direction to the magnetometers, i.e., the borehole axis. In this orientation (θ is 0° or 180°), the magnet's field is a maximum and installation is simplified. Figure 5 shows how the magnet and magnetometers, strapped to a common insertion tool/grout pipe, would appear in a borehole. For a given borehole diameter, this configuration allows the largest possible magnets to be used.*

The field of a dipole varies inversely as the cube of distance. Given the finite size of the earth's field and the magnetometer noise, this means that the closest magnets will be best resolved in position. With 3.8 x 22.9 cm (1.5 x 9 inch) magnets as used for MIGHTY EPIC, we would probably want the installed magnet to magnetometer separation to be no more than about 1 meter to insure differential displacement determinations to within about five centimeters.

A critical requirement for the success of the technique is the clean recording of all six magnetometer signals. The loss of even one channel would seriously hamper interpretation of the remaining signals. However, with six good records, all five possible motions of the magnet would be observed and we would have some indication of possible rotations of the magnetometers. Thus, a fairly complete measurement of the vector block motion would occur.

*The magnetic strength of a cylindrical permanent Alnico magnet increases linearly with its volume for a fixed length to diameter ratio. This ratio must be at least six to maximize the dipole moment for a given magnet volume.

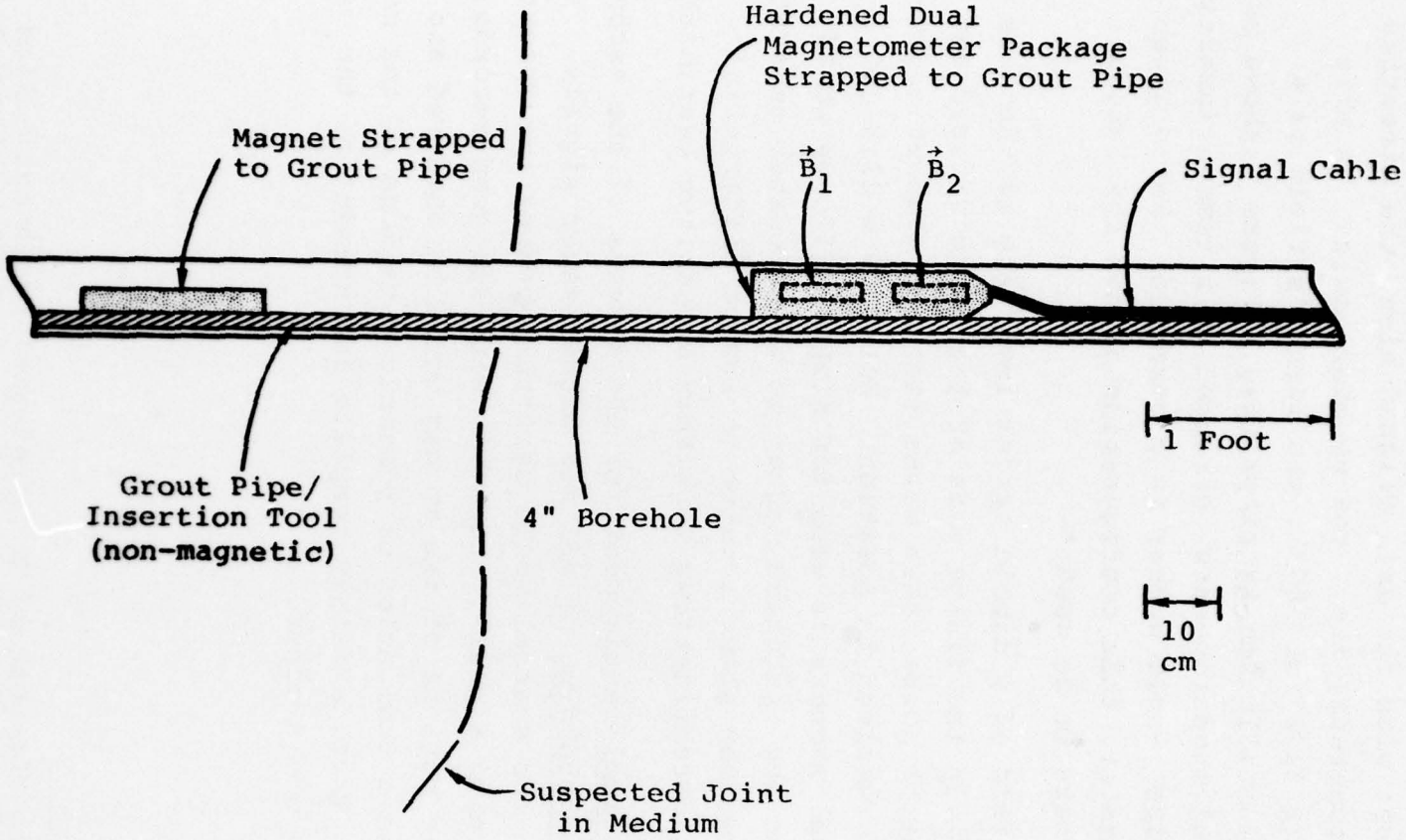

Figure 5. Section view of magnet-magnetometers installed in a borehole.

Clearly, this technique is not trivial to implement. However, the alternatives also have limitations. Integrations of accelerometer or velocity gauge signals are required to derive displacement. The accurate records from two such gauges are needed to calculate the differential block motion in each Cartesian coordinate. Rotary motion is quite difficult to observe with velocity transducers. The use of a completely different set of physical principles makes the magnetic scheme attractive. The "gradiometer" approach offers an excellent alternative and complement to the usual ground motion sensors for the study of block motion.

REFERENCES

1. P. L. Coleman (1978), "MIGHTY EPIC Interface Experiment," Draft report submitted May, 1978.

2. D. R. Grine and P. L. Coleman (1974), "Ground Motion Gauge Development," DNA Report No. 3524T (Final).

DISTRIBUTION LIST

DEPARTMENT OF DEFENSE

Assistant to the Secretary of Defense
Atomic Energy
ATTN: Executive Assistant

Defense Advanced Rsch. Proj. Agency
ATTN: TIO
ATTN: NMRO
ATTN: PMO
ATTN: STO

Defense Documentation Center
12 cy ATTN: TC

Defense Nuclear Agency
ATTN: DDST
ATTN: SPTD
2 cy ATTN: SPSS
4 cy ATTN: TITL

Field Command
Defense Nuclear Agency
ATTN: FCTMOF
ATTN: FCT
ATTN: FCPR

Livermore Division Fld. Command DNA
Department of Defense
ATTN: FCPRL

NATO School (SHAPE)
ATTN: U.S. Documents Officer

DEPARTMENT OF THE ARMY

Deputy Chief of Staff for Rsch. Dev. & Acq.
Department of the Army
ATTN: DAMA-AOA-M

Harry Diamond Laboratories
Department of the Army
ATTN: DELHD-TI
ATTN: DELHD-NP

U.S. Army Ballistic Research Labs.
ATTN: DRXBR-X, J. Meszaros
ATTN: Technical Library

U.S. Army Engr. Waterways Exper. Station
ATTN: Library
ATTN: F. Hanes
ATTN: J. Ingram

U.S. Army Materiel Dev. & Readiness Cmd.
ATTN: DRXAM-TL

DEPARTMENT OF THE NAVY

Civil Engineering Laboratory
ATTN: Code L08A

David W. Taylor Naval Ship R&D Ctr.
ATTN: Code L42-3

DEPARTMENT OF THE NAVY (Continued)

Naval Facilities Engineering Command
ATTN: Code 09M22C

Naval Ship Engineering Center
ATTN: Code 09G3

Naval Surface Weapons Center
ATTN: Code F31

Office of Naval Research
ATTN: Code 715

DEPARTMENT OF THE AIR FORCE

Air Force Institute of Technology, Air University
ATTN: Library

Air Force Weapons Laboratory, AFSC
ATTN: SUL
ATTN: DES-S, M. Plamondon
ATTN: DEX, J. Renick
ATTN: DEX

Assistant Chief of Staff
Intelligence
Department of the Air Force
ATTN: INATA

DEPARTMENT OF ENERGY

Department of Energy
ATTN: Doc. Con. for Technical Library

Department of Energy
ATTN: Doc. Con. for Classified Library

Department of Energy
ATTN: Doc. Con. for Technical Library

Lawrence Livermore Laboratory
ATTN: Doc. Con. for Technical Information
Dept. Library

Sandia Laboratories
ATTN: Doc. Con. for Library & Security
Classification Div.

Sandia Laboratories
ATTN: Doc. Con. for A. Chaban
ATTN: Doc. Con. for L. Vortman
ATTN: Doc. Con. for 3141

OTHER GOVERNMENT AGENCY

National Bureau of Standards
ATTN: P. Lederer

DEPARTMENT OF DEFENSE CONTRACTORS

Aerospace Corp.
ATTN: Technical Information Services
ATTN: P. Mathur

DEPARTMENT OF DEFENSE CONTRACTORS (Continued)

Agbabian Associates
ATTN: M. Agbabian

Artec Associates, Inc.
ATTN: D. Baum

Civil/Nuclear Systems Corp.
ATTN: J. Bratton

EG&G Washington Analytical Services Center, Inc.
ATTN: Library

Electromechanical Sys. of New Mexico, Inc.
ATTN: R. Shunk

General Electric Company—TEMPO
Center for Advanced Studies
ATTN: DASIAC

H-Tech. Laboratories, Inc.
ATTN: B. Hartenbaum

ITT Research Institute
ATTN: Documents Library

Kaman Sciences Corp
ATTN: D. Sachs
ATTN: Library

Merritt CASES, Inc.
ATTN: J. Merritt
ATTN: Library

Newmark, Nathan M.
Consulting Services
ATTN: N. Newmark
ATTN: W. Hall

DEPARTMENT OF DEFENSE CONTRACTORS (Continued)

Physics International Co.
ATTN: C. Vincent
ATTN: F. Sauer/C. Godfrey
ATTN: Technical Library

R&D Associates
ATTN: Technical Information Center
ATTN: C. Knowles/J. Lewis
ATTN: C. MacDonald

Science Applications, Inc.
ATTN: Technical Library

Southwest Research Institute
ATTN: W. Baker

SRI International
ATTN: B. Gasten/P. DeCarli
ATTN: G. Abrahamson

Systems, Science & Software, Inc.
ATTN: D. Grine
ATTN: Library
ATTN: P. Coleman

TRW Defense & Space Sys. Group
ATTN: Technical Information Center
2 cy ATTN: P. Dai

TRW Defense & Space Sys. Group
ATTN: E. Wong

Wang, Eric H.
Civil Engineering Rsch. Fac.
ATTN: N. Baum

Weidlinger Assoc., Consulting Engineers
ATTN: M. Baron

Weidlinger Assoc., Consulting Engineers
ATTN: J. Isenberg